JOURNAL OF SOLID STATE CHEMISTRY 72, 42–51 (1988)

A Low-Temperature Powder Neutron Diffraction Study of the Antiferromagnetic Phase of $Mn_xCo_{1-x}O$*

D. A. O. HOPE** AND A. K. CHEETHAM

University of Oxford, Chemical Crystallography Laboratory, 9 Parks Road, Oxford OX1 3PD, United Kingdom

Received February 24, 1987

High-resolution powder neutron diffraction measurements have been used to study the crystallographic and magnetic properties of antiferromagnetic $Mn_xCo_{1-x}O$. Both the lattice and magnetic parameters reveal three distinct regions of behavior across the range of composition, which can be attributed to changes in the relative proportions of Co^{2+} ions adopting the alternative $^4A_{2g}$ and ^4E_g ground states. These modifications are brought about by an exchangestrictive lowering of symmetry due to Mn^{2+}–Mn^{2+} nearest-neighbor interactions. In the cobalt-rich ($x < 0.36$) regime, the orbital moments of some Co^{2+} ions are quenched and distortions characteristic of both Jahn–Teller and magnetostrictive stabilizations are observed. For $0.51 < x < 0.66$, spin-only Co^{2+} moments and solely Jahn–Teller distortions are evident. When Mn^{2+} is in large excess, indications of a magnetostrictive distortion due to Co^{2+} appear; here the Co^{2+} concentration may be insufficient to sustain a cooperative Jahn–Teller distortion. These results allow a new model for the electronic structure of Co^{2+} in CoO, involving noncollinear spin and orbital angular momenta, to be proposed.

Introduction

We have recently undertaken an extensive study of the magnetic and structural properties of the antiferromagnetic phases of the binary solid solutions involving the transition metal monoxides MnO, Fe_zO, CoO, and NiO. In the paramagnetic phases, all of these oxides have the rock-salt structure, but become magnetically ordered below Néel temperatures which range from 118 K (MnO) to 523 K (NiO). Here, the type II antiferromagnetic structure is adopted, in which the spin directions of alternate ferromagnetic (111) planes are reversed. The transition metal ions all exhibit magnetic moments which are relatively close to the spin-only values, ranging from 1.8 μ_B (Ni^{2+}: $S = 1/2$) to 4.6 μ_B (Mn^{2+}: $S = 5/2$). However, incomplete quenching of the orbital angular momenta of Fe^{2+} and Co^{2+} maintains an orbital contribution to the moment in Fe_zO and CoO. The former is further complicated by the inherent nonstoichiometry. The principal differences in magnetic properties between the four oxides arise from the presence, or otherwise, of the orbital contribution; this determines the type of crystallographic distortion in the

* Dedicated to Professor J. B. Goodenough on his 65th birthday.

** Present address: Royal Signals and Radar Establishment, St. Andrews Road, Great Malvern, Worcs WR14 3PS, U.K.

0022-4596/88 $3.00

antiferromagnetic phase, and the direction and anisotropy of the magnetic moment.

Of the two components of the $Mn_xCo_{1-x}O$ solid solution, MnO shows somewhat more straightforward behavior. Here, the magnetic moments are restricted to the ferromagnetic (111) easy planes by magnetic dipole forces (*1*), although the easy axes within these planes have yet to be determined. MnO also experiences a relatively large trigonal ($\alpha > 90°$) exchangestriction below T_N (*2*), which is due to direct nearest-neighbor cation–cation superexchange. However, CoO undergoes a large tetragonal contraction ($c/a > 1$) (*3*), as a consequence of the residual, unquenched orbital angular momentum of octahedrally coordinated high spin Co^{2+}. The threefold orbital degeneracy can be relieved by either a uniaxial (tetragonal, $c/a > 1$ or trigonal, $\alpha < 90°$), cooperative Jahn–Teller (J.T.) distortion to a $^4A_{2g}$ state or, in the presence of a molecular field, by a trigonal ($\alpha > 90°$) or tetragonal ($c/a < 1$) Jahn–Teller distortion to a ^4E_g state. This is further stabilized by spin–orbit (S.O.) coupling and a Zeeman hyperfine interaction in the internal magnetic field (*4*). The latter possibility (J.T. + S.O.: $c/a < 1$) occurs in CoO, and in this case the spin moment is linked to the axis of deformation, giving rise to deformation-dependent single ion (magnetoelastic) anisotropy energy (*5*).

The sublattice magnetization vector in CoO lies approximately parallel to [113] (*6*), i.e., 27° from the c axis and 8° out of the (111) plane. This result has been the source of much discussion since the magnetoelastic coupling energy is presumed to be the dominant anisotropic effect and, in the presence of weak trigonal terms such as the magnetic dipole interaction, favors an easy axis close to [001] (*5*). In an attempt to resolve this paradox, an alternative four k-vector magnetic structure has been proposed (*6*) and defended (*7*, *8*), but X-ray data (*3*) and a recent single-crystal neutron experiment under uniaxial compression (*9*) indicate that CoO indeed has a collinear, single-axis moment arrangement. This is also the conclusion of the latest theoretical work on the subject (*10*) which, in addition, suggests that an anisotropic cation–cation superexchange term is responsible for the unusual moment direction. However, the situation is further complicated by some NMR results (*11*) which indicate that the hyperfine field is 21.1 ± 0.5° from [001]. They then deduce that the spin and orbital angular momenta are noncollinear with the latter inclined at 22.8° to the c axis.

The majority of previous work on antiferromagnetic MnO–CoO has been limited to magnetic susceptibility (*12*) and specific heat measurements (*13*). These show that $T_N(x)$ is an approximately linear function, as predicted by molecular field theory (*12*), where the next-nearest-neighbor exchange constant between unlike ions is the geometric mean of that between like ions. Together with the large Néel temperatures, this behavior indicates that the 180° cation–oxide–cation superexchange interactions are appreciable. It is also consistent with our work on the antiferromagnetic phases of $Co_xNi_{1-x}O$ (*14*), $Mn_xNi_{1-x}O$ (*15*), and $(Mn_xFe_{1-x})_zO$ (*16*), which indicate that the magnetic structures are collinear. Therefore, no "oblique ferromagnetic" phase analogous to that observed in random two-dimensional antiferromagnets such as $Fe_xCo_{1-x}Cl_2$ (*17*), $K_2Fe_xMn_{1-x}F_4$ (*18*), and $K_2Co_xFe_{1-x}F_4$ (*19*) is evident in these mixed three-dimensional systems. Antiferromagnetic resonance (AFMR) spectra have been measured for $Mn_xCo_{1-x}O$ with $0.94 < x < 1.0$ (*20*) and show features similar to those observed in an AFMR study of $Co_xNi_{1-x}O$ (*21*). The anisotropy constant derived, 32.8 cm^{-1}/ion, compares well with the magnetoelastic coupling energy of Co^{2+} calculated by Kanamori (*5*) and on this basis it seems that the single-ion anisotropy of Co^{2+} is again an important factor.

Experimental

The mixed crystals were prepared either by a conventional high-temperature, solid state route or by a coprecipitation method. In the first, appropriate amounts of MnO and CoO were mixed together in an agate mortar, pelleted, and fired at 1000°C for 24 hr, using a static CO_2 atmosphere. The firings were repeated until adequate sample homogeneities were obtained, as assessed by X-ray Guinier photography and analytical electron microscopy (*22*). The Mn : Co ratios were checked by atomic absorption spectrometry. MnO was synthesized in a Mullite tube by decomposing manganous oxalate under a stream of hydrogen at 1000°C. CoO was prepared by firing cobaltous carbonate under a stream of CO_2 at 500°C for 4 hr and then at 1000°C *in vacuo* for a further 24 hr.

Alternatively, aqueous solutions of $MnCl_2 \cdot 4H_2O$ and $Co(NO_3)_2 \cdot 6H_2O$ were mixed to give the required proportions of the two ions. The resulting solution was added with stirring to an excess of saturated $KHCO_3$ at 80°C, and the suspension was filtered, washed well with water, and dried. The mixed carbonate was fired under a stream of CO_2 at 600°C, and the homogeneity and average particle size were improved by firing at 1000°C under a static CO_2 atmosphere for a further 24 hr.

TABLE I

SPACE GROUPS AND COORDINATES EMPLOYED IN STRUCTURAL REFINEMENTS

$P\bar{1}$	Metal at 0, 0, 0 (1a)
	Oxygen at 0, 0, 1/2 (1b)
$C2/m$	Metal at 0, 0, 0 (2a)
	Oxygen at 0, 1/2, 1/2 (2d)
$R\bar{3}$	Metal at 0, 0, 0 (3a)
	Oxygen at 0, 0, 1/2 (3b)
$Fm3m$	Metal at 0, 0, 0 (4a)
	Oxygen at 1/2, 1/2, 1/2 (4b)

Powder neutron diffraction data at 5 K were collected for MnO, CoO, and seven solid solution samples on the ten-counter D1A diffractometer at the ILL, Grenoble, using wavelengths of 1.510 and 1.904 Å. The 8-g samples were held in vanadium cans of 10 mm diameter, which were located in a vanadium-tailed cryostat, and the time for a complete scan ($0° < 2\theta < 160°$) varied from 12 to 24 hr. Variable temperature measurements of the magnetic (111) and certain nuclear peaks of two samples were also accomplished. The data were analyzed by the Rietveld profile analysis technique (*23*) on the basis of a distorted rock-salt structure, or component cells of $R\bar{3}$, $C2/m$, and $P\bar{1}$ symmetry. The appropriate space group coordinates are given in Table I and refer to the cell parameters shown in Table II. Where it was more

TABLE II

LATTICE PARAMETERS, OVERALL TEMPERATURE FACTORS, AND R VALUES FOR $Mn_xCo_{1-x}O$ at 5 K (STANDARD DEVIATION IN PARENTHESES)

Composition	λ (Å)	a (Å)	b (Å)	c (Å)	α (deg)	β (deg)	γ (deg)	B overall (Å^2)	R_{nuc}	R_{mag}	R_{pr}
CoO	1.904	8.5204(2)	8.5204(2)	8.4150(2)	90	90	90	−0.21(4)	1.59	4.75	5.56
	1.904	5.1738(9)	3.0119(1)	6.0258(14)	90	54.413(10)	90	−0.19(3)	1.54	3.22	4.89
$Co_{0.95}Mn_{0.05}O$	1.513	8.5477(11)	8.5299(11)	8.4535(7)	90	90	90	0.15(5)	4.52	4.35	8.63
$Co_{0.90}Mn_{0.10}O$	1.904	3.0096(2)	3.0086(2)	6.0104(5)	60.327(6)	90.467(2)	60.288	−0.23(4)	3.25	3.55	5.96
$Co_{0.75}Mn_{0.25}O$	1.511	3.0386(4)	3.0387(2)	6.0693(7)	60.139(9)	90.368(4)	60.154	0.29(2)	2.62	3.84	5.83
$Co_{0.64}Mn_{0.36}O$	1.512	3.0609(3)	3.0599(2)	6.1090(5)	60.052(8)	90.299(4)	60.085	0.34(2)	3.38	2.75	6.15
$Co_{0.49}Mn_{0.51}O$	1.513	5.3341(4)	3.0804(2)	6.1340(3)	90	54.767(4)	90	0.62(2)	3.57	2.82	7.04
$Co_{0.33}Mn_{0.67}O$	1.511	5.3789(9)	3.1030(2)	6.1678(9)	90	54.608(9)	90	0.32(2)	2.92	4.08	6.07
	1.904	5.3674(3)	3.0973(2)	6.1557(2)	90	54.602(3)	90	0.30(2)	1.73	3.61	5.16
$Co_{0.17}Mn_{0.83}O$	1.512	5.4234(7)	3.1297(4)	6.2040(7)	90	54.449(8)	90	0.25(2)	3.16	7.75	8.23
	1.512	5.4206(6)	3.1311(3)	6.2127(6)	90	54.334(7)	90	0.26(2)	3.22	3.25	7.35
MnO	1.513	3.1536(1)	3.156(1)	15.2056(4)	90	90	120	0.25(2)	2.77	2.75	7.04

TABLE III

EQUIVALENT PSEUDOCUBIC CELLS FOR $Mn_xCo_{1-x}O$ at 5 K

Sample	a (Å)	b (Å)	c (Å)	α (deg)	β (deg)	γ (deg)
CoO	(b) 8.520	8.520	8.415	89.98	89.98	89.98
$Co_{0.90}Mn_{0.10}O$	8.541	8.554	8.471	89.96	90.08	90.01
$Co_{0.75}Mn_{0.25}O$	8.616	8.605	8.561	90.15	90.08	90.05
$Co_{0.64}Mn_{0.36}O$	8.671	8.650	8.626	90.22	90.12	90.09
$Co_{0.49}Mn_{0.51}O$	8.693	8.693	8.714	90.09	90.09	90.24
$Co_{0.33}Mn_{0.67}O$	(a) 8.750	8.750	8.770	90.29	90.29	90.36
	(b) 8.733	8.733	8.751	90.29	90.29	90.36
$Co_{0.17}Mn_{0.83}O$	(a) 8.813	8.813	8.826	90.47	90.47	90.51 ($c/a > 1$)
	(b) 8.821	8.821	8.808	90.50	90.50	90.45 ($c/a < 1$)
MnO	8.864	8.864	8.864	90.61	90.61	90.61

convenient to use reduced cells, the corresponding pseudocubic lattice parameters are set out in Table III.

The scattering lengths of Mn, Co, and O were taken from Bacon (*24*) and the form factors determined previously for MnO and CoO (*25, 7*) were applied to the magnetic peaks of these data sets. Initially, the magnetic form factors applied to the solid solution data were calculated according to a linear interpolation between the MnO and CoO curves. The degree of expansion or contraction of either curve was then varied empirically so as to minimize the profile reliability index. This procedure was necessary since the magnitudes of a variety of factors which affect the form factor, for example, covalency and the orbital magnetic moment, are unknown in the solid solutions. Peaks occurring at $2\theta < 25°$ were omitted from the analyses owing to the large deviations from the Gaussian peak shape at these angles. An asymmetry correction was applied in the range $25° < 2\theta < 48°$, but no absorption correction was made. Table II shows that two samples, CoO and $Co_{0.90}Mn_{0.10}O$, exhibited negative temperature factors due to absorption by cobalt (*26*). We can be confident that the neglect of the absorption correction has no significant effect on the parameters of interest since the magnetic and structural information derived for CoO is in excellent agreement with that obtained in previous work (*3, 6*). Figure 1 indicates the level of agreement between observed and calculated profiles for two compositions.

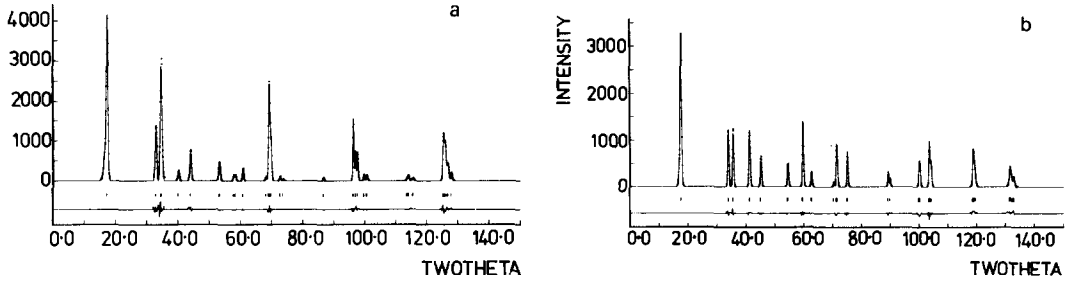

FIG. 1. Observed (points) and calculated (solid line) profiles of (a) $Mn_{0.83}Co_{0.17}O$ and (b) $Mn_{0.25}Co_{0.75}O$ at 5 K.

Structural Parameters at 5 K

Trigonal Exchangestrictions

The first two rows of Table II indicate that refinements of the CoO data according to monoclinic cell parameters yielded somewhat better results than a cell restricted to the three-parameter (tetragonal) case. The equivalent pseudocubic cell is shown in Table III. The small angular distortion has not been observed before by neutron diffraction, although Saito *et al.* came to a similar conclusion using X-ray diffraction (*3*).

In MnO–NiO (*15*), the $\alpha > 90°$ exchangestriction due to Mn^{2+}–Mn^{2+} interactions is opposed by a trigonal distortion of opposite sign emanating from the Mn^{2+}–Ni^{2+} exchange. A similar effect is not evident here since, as Fig. 2 shows, the average trigonal distortion develops smoothly with increasing manganese content. Consequently, the Mn^{2+}–Co^{2+} interactions appear to be weak when compared with the Mn^{2+}–Mn^{2+} exchange. A slight anomaly occurs in the vicinity of the 50 : 50 composition, which may be caused by a (masked) trigonal J.T. ($\alpha < 90°$) stabilization of some Co^{2+} ions. However, despite the trigonal bias of the exchangestriction this is not a major effect. It is noteworthy that a macroscopic exchangestriction is not observed in $Mn_{0.05}Co_{0.95}O$, but it is likely that local distortions stemming from the cation–

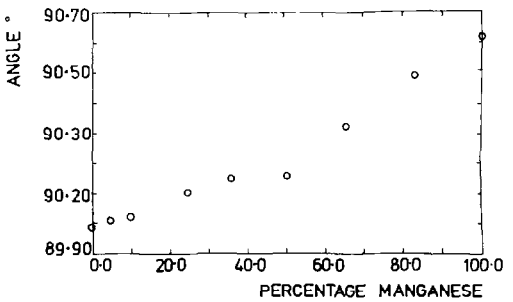

FIG. 2. Dependence of the rhombohedral distortion of $Mn_xCo_{1-x}O$ on composition.

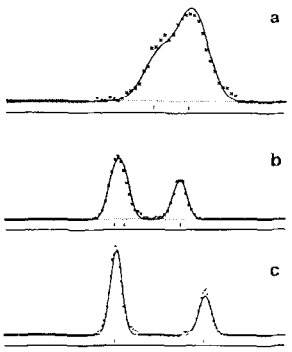

FIG. 3. Pseudocubic {800} peaks of (a) $Mn_{0.67}Co_{0.33}O$, (b) $Mn_{0.10}Co_{0.90}O$, and (c) CoO. Reflection positions are marked.

cation exchange remain important, as is discussed in the next section.

Pseudocubic Axial Lengths

The overall symmetries of the solid solutions (Tables II and III) can be explained on the basis of an exchangestriction of trigonal symmetry superimposed upon one or two mutually perpendicular tetragonal distortions. The overall crystal class then changes from monoclinic–orthorhombic–triclinic–monoclinic–trigonal on crossing the phase diagram from CoO to MnO. In CoO, the $c/a < 1$ distortion causes the {800} peak to split into two components with intensity ratio 2 : 1. A tetragonal contraction is also indicated by the best refinement for $Mn_{0.83}Co_{0.17}O$ (Table II), although the resolution is insufficient to produce any observable splitting of the {800} peak. In the broad region between these compositions, the dramatic variations in the axial lengths a, b, and c (as given in Table III) can be readily assessed from Fig. 3. The relative sizes of a, b, and c conform to the following pattern: for 5–25% MnO, $a > b \gg c$; for $Mn_{0.36}Co_{0.64}O$, $a > b > c$; and for 51–67% MnO, $a = b > c$ ($c/a > 1$).

When the alternative methods of stabilization of a Co^{2+} site (discussed in the Introduction) are considered, it is evident

that, with increasing manganese content up to $Mn_{0.67}Co_{0.33}O$, the cooperative elastic J.T. case (leading to a $^4A_{2g}$ ground state) decreases in energy in comparison with the magnetoelastic J.T. + S.O. situation found in CoO. For small concentrations of Mn^{2+} in $Mn_xCo_{1-x}O$, triclinic or, when the overall trigonal exchangestriction is unobservable, orthorhombic structures are found, in which the J.T. + S.O. magnetostriction ($c/a < 1$) and J.T. distortion ($c/a > 1$) coexist. These deformations are directed along different principal axes, producing the low symmetries observed. The magnetostriction is not detected for $0.51 < x < 0.67$, but the cooperative elastic coupling is sufficient to sustain the J.T. distortion, leading to monoclinic symmetry when combined with the trigonal exchangestriction. It is interesting to note, however, that the $x = 0.67$ sample is probably below the percolation limit for Co^{2+} in the rock-salt lattice (*27*).

Presumably, the pseudotetragonal contraction of $Mn_{0.83}Co_{0.17}O$ is found because the cobalt concentration is too small to support a cooperative J.T. distortion of the octahedral sites occupied by cobalt, and because the average symmetry is higher owing to the large excess of manganese. It is noteworthy that this result is consistent with some AFMR data, which require that the orbital angular momentum of Co^{2+} reemerges for $0.94 < x < 1.0$ (*20*).

The behavior as a function of composition can be explained in terms of an increase in the range of local symmetries experienced by the Co^{2+} ions. This effect then limits the number of cobaltous ions having an orbital contribution. There are two possible factors which control the lowering of symmetry. First, the presence of Mn^{2+} in the n.n. cation positions around Co^{2+} lowers the point symmetry; this effect has been clearly demonstrated in $(Mn_xFe_{1-x})_zO$ (*28*), in which Fe^{2+} experiences a broader distribution of electric field gradients, according to Mössbauer spectroscopy. Second, the n.n exchange interactions (predominantly cation–cation) between like and unlike ions are sensitive to changes in ionic separation (cf. the large exchangestriction in MnO) and lead to local site distortions. We believe that the first of these factors has a minor influence since $Co_xNi_{1-x}O$ shows no evidence for quenched Co^{2+} orbital angular momenta (*14*). The dominant factor appears to be the presence of cation–cation interactions (Co^{2+}–Co^{2+}, Co^{2+}–Mn^{2+}, Mn^{2+}–Mn^{2+}) leading to exchangestrictions of different magnitudes. As discussed at the beginning of the previous section, the first two are small while the latter is large, and so the particular environment of a Co^{2+} ion is likely to be somewhat distorted if an unequal and asymmetric Co^{2+}/Mn^{2+} distribution occurs. If these distortions affect the dispositions of the oxide ligands sufficiently, the associated crystal field splittings will quench the residual orbital angular momentum associated with the ^4E_g state. In the midrange of composition, the symmetry is low enough to strongly favor the J.T. stabilization.

From the relative sizes of a, b, and c, it seems that the proportion of J.T. Co^{2+} ions does not increase substantially up to the $x = 0.25$ composition. In $Mn_{0.36}Co_{0.64}O$, the equal separations of a, b, and c then signify that the transition of $c/a > 1$ is more advanced, and this is complete by $x = 0.51$. Presumably, a minimum number of manganous ions in the first coordination sphere of the majority of Co^{2+} ions is necessary to induce the transition to the case where the majority of ions show a J.T. stabilization. However, the results for $Mn_{0.05}Co_{0.95}O$ show that only a small amount of manganese is necessary to quench the orbital momenta of a sizable number of cobaltous ions; the ease with which the electronic structure of Co^{2+} can be changed will be discussed further in the final section of the paper.

Magnetic Parameters at 5 K

The four regions of behavior identified from the lattice parameter measurements are again evident in a plot of the average sublattice moments against composition (Fig. 4). Here, the solid lines join the moment of MnO with that of CoO and a hypothetical oxide containing a spin-only $S = 3/2$ ion whose moment is reduced somewhat by covalency. It should be emphasized that any deductions from these data depend upon the assumption that approximate collinearity of the moments of different ionic species is maintained in all samples owing to the large 180° superexchange. The validity of this assertion is borne out by much other evidence (*27*). Consequently, compositions between 5 and 36% manganese show a reduction from the upper line, indicating that a proportion of the individual Co^{2+} orbital momenta have been quenched, while the moments of $Mn_{0.51}Co_{0.49}O$ and $Mn_{0.67}Co_{0.33}O$ tend toward the lower line. This is in agreement with the Jahn–Teller ($c/a > 1$) distortions of these samples. The consistency of the comparison between the magnetic moment and lattice parameter values is also demonstrated by the moments of the 5–25% MnO samples, which fall approximately on another straight line. This suggests that they involve similar degrees of quenching; here, it will be recalled, the difference between

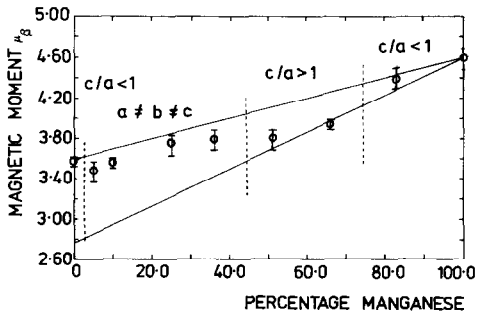

FIG. 4. Mean sublattice moments of $Mn_xCo_{1-x}O$ at 5 K.

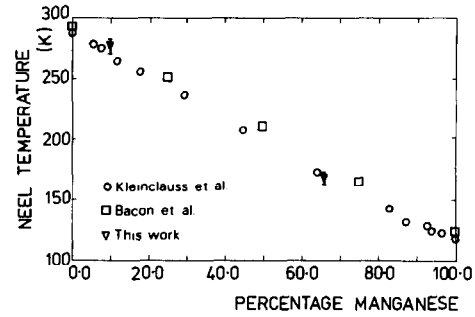

FIG. 5. Composition dependence of the Néel temperature in $Mn_xCo_{1-x}O$.

the cell parameters a and b is approximately constant and much smaller than that between b and c. The decrease in the moment caused by the incorporation of as little as 5% MnO into CoO should also be stressed.

The profile analyses of the magnetic peaks at all compositions indicate that the magnetic vectors lie close to, or within, the pseudocubic (111) plane. In CoO, the moment is found to be approximately 26° from [001], in agreement with previous work (for example, Van Laar (*6*)). However, the magnetic peaks of the solid solutions are not well resolved, and by comparison with CoO the corresponding sublattice magnetization directions can be determined less conclusively. In addition, it remains possible that the moments do not adopt a rigidly fixed orientation owing to the random natures of the solid solutions.

Variable Temperature Experiments

The {111} magnetic peaks of two samples containing 10 and 67% manganese were monitored as a function of increasing temperature and extrapolated to zero intensity to give the Néel temperatures plotted in Fig. 5. The values compare well with those derived by other techniques (*12, 13*). In order to study the temperature variations of the tetragonal and trigonal distortions, the

pseudocubic {800} and {444} nuclear peaks of $Mn_{0.67}Co_{0.33}O$ were scanned up to, and above, the Néel temperature. Accurate profile analyses were achieved at each point after summing over three counters of the diffractometer. Both the trigonal exchangestriction and the J.T. and J.T. + S.O. tetragonal distortions should vary with temperature in the same manner as the sublattice magnetization (*29*), and this is observed in MnO (*2*) and for the magnetostriction due to Co^{2+} in $Co_xNi_{1-x}O$ (*14*). A similar function is adopted by the trigonal distortion of $Mn_{0.67}Co_{0.33}O$ (Fig. 6), but the same figure indicates that the variation of c/a with temperature does not have the expected form. Most noticeably, no tetragonality is observed at 5 K below T_N, although a marked trigonal distortion has developed at this temperature. This observation, together with the unusual shape of the curve at low temperatures, suggests that the intersite correlations necessary for the $c/a > 1$ J.T. distortion may be induced by a small amount of magnetoelastic coupling which increases slightly with diminishing temperature. The need for an additional mechanism to support the J.T. distortion, other than cooperative elastic coupling, could be a consequence of the metal : metal ratio in this particular sample ($Co^{2+} : Mn^{2+} = 0.33 : 0.67$). Here, the proportion of cobalt is probably below the percolation limit for the rock-salt structure. This quantity can be estimated from a variety of experiments; for example, in spinel solid solutions containing Mn^{3+}, the limiting composition (x_t) for the cooperative J.T. distortion varies from 0.4 to 0.73 (*30*). In $Ni_xMg_{1-x}O$ (*31, 32*), no long-range magnetic order occurs for $x_t < 0.4$.

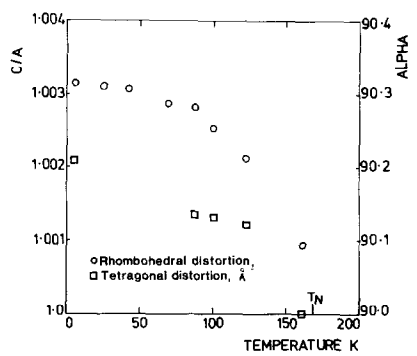

FIG. 6. Temperature variations of the rhombohedral and tetragonal distortions of $Mn_{0.67}Co_{0.33}O$.

A Comment on the Electronic Structure of Co^{2+} in CoO

The complicated variations in the magnetic and structural parameters of $Mn_xCo_{1-x}O$ with composition have been rationalized in terms of the effect of local site symmetry on the number of Co^{2+} ions possessing an orbital magnetic moment and of the concentration dependence of the cooperative elastic coupling between cobaltous ions in the $^4A_{2g}$ state. These factors are sufficient to explain all the behavior observed, but it seems surprising that the perturbations due to manganese when $x = 0.05$ cause a significant number of Co^{2+} ions to adopt the quenched configuration. This may suggest that the ^4E_g and $^4A_{2g}$ states of Co^{2+} in CoO are comparable in energy, despite the favorable spin–orbit and magnetoelastic coupling terms associated with the E state. A contributory factor to this situation could be a reduction in spin–orbit coupling due to noncollinear S and L as suggested by the NMR work of Okada and Yasuoka (*11*). In their paper, the magnetic moment is equated with the spin direction, from which a value of 22.8% for the inclination of the orbital moment to [001] is derived. However, we should point out that neutron diffraction does not reveal the spin direction when the spin and orbital momenta are noncollinear. We can then propose a new model in agreement with both NMR and neutron data. This involves an orbital moment parallel to the tetragonal axis of deformation, which maximizes the

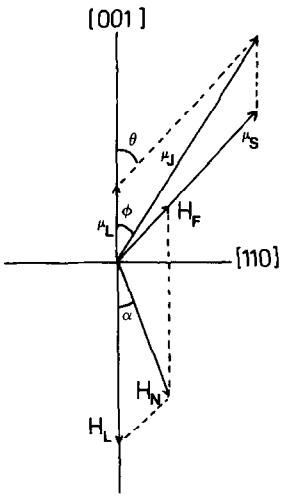

FIG. 7. Vector diagram showing a possible noncollinear arrangement of the spin and orbital angular momenta of CoO. μ_S, μ_L, and μ_J are the spin, orbital, and total angular momentum vectors, and H_N, H_F, and H_L are the observed, Fermi contact, and orbital hyperfine fields, respectively.

magnetoelastic coupling energy and is consistent with the substantial tetragonal distortion observed. The spin moment is then allowed to adopt any orientation toward the (111) plane. As long as the angle, θ, between the two vectors is not too large, the spin–orbit coupling energy is only slightly reduced owing to the $\cos\theta$ term in the scalar product of S and L.

The data of Okada and Yasuoka (*11*) are reinterpreted in Fig. 7 for comparison with the model outlined above. A total hyperfine field of +498 MHz at $\alpha = 21.1°$ to [001] can have components $H_L = +660$ MHz along [001] and $H_F = -264$ MHz at $\theta = 43°$ to [001]. The value of H_F was calculated by Okada and Yasuoka, and their estimate of H_L (+724 MHz) is close to that derived here. Combination of a spin moment of $gS = 2.7\ \mu_B$ (reduced by covalency from 3 μ_B) in the direction of H_F, and an orbital moment of 1 μ_B parallel to [001] then results in a magnetic moment of 3.5 μ_B inclined at $\phi = 31.7°$ to the fourfold axis (in excellent agreement with the neutron diffraction results).

There are a number of many-atom effects present in the crystal, but not in the free ion, which might account for the decoupling of L and S and placement of S close to the (111) plane. In addition to the magnetoelastic coupling, anisotropic exchange (*10*), the magnetic dipole interaction (*1*), and the reduction of the spin–orbit coupling constant by covalency (*33*) can be cited.

Acknowledgments

The authors are indebted to Professor J. B. Goodenough and Dr. P. D. Battle for some helpful comments, and to Drs. A. W. Hewat, C. Wilkinson, J. L. Buevoz, and S. Heathman of the ILL for experimental assistance. They also acknowledge the provision of neutron facilities and a research studentship (D.A.O.H.) by the SERC (U.K.).

References

1. J. I. KAPLAN, *J. Chem. Phys.* **22,** 1709 (1954).
2. B. MOROSIN, *Phys. Rev. B* **1,** 236 (1970).
3. S. SAITO, K. NAKAHIGASHI, AND Y. SHINOMURA, *J. Phys. Soc. Japan* **21,** 850 (1966).
4. J. B. GOODENOUGH, *Phys. Rev.* **171,** 466 (1968).
5. J. KANAMORI, *Prog. Theor. Phys. (Kyoto)* **17,** 197 (1957).
6. B. VAN LAAR, *Phys. Rev.* **138,** A854 (1965).
7. D. C. KHAN AND R. A. ERICKSON, *Phys. Rev. B* **1,** 2243 (1970).
8. E. F. BERTAUT, *J. Phys. Chem. Solids* **30,** 763 (1969).
9. D. HERRMANN-RONZAUD, P. BURLET, AND J. ROSSAT-MIGNOD, *J. Phys. C.* **11,** 2123 (1978).
10. T. YAMADA AND O. NAKANISHI, *J. Phys. Soc. Japan* **36,** 1304, 1315 (1974).
11. K. OKADA AND H. YASUOKA, *J. Phys. Soc. Japan* **43,** 34 (1977).
12. G. E. BACON, R. STREET, AND R. H. TREDGOLD, *Proc. R. Soc. A* **217,** 252 (1953).
13. J. KLEINCLAUSS, R. MAINARD, H. FOUSSE, N. CIRET, D. BOUR, AND A. J. POINTON, *J. Phys. C* **14,** 1163 (1981).
14. P. D. BATTLE, A. K. CHEETHAM, AND G. A. GEHRING, *J. Appl. Phys.* **50,** 7578 (1979).
15. A. K. CHEETHAM, AND D. A. O. HOPE, *Phys. Rev. B* **27,** 6964 (1983).

16. G. J. LONG, D. A. O. HOPE, AND A. K. CHEETHAM, *Inorg. Chem.* **23,** 3141 (1984).
17. T. TAWARAYA AND K. KATSUMATA, *Solid State Commun.* **32,** 337 (1979).
18. L. BEVAART, E. FRIKKEE, J. V. LEVESQUE, AND L. J. DE JONGH, *Phys. Rev. B* **18,** 3376 (1978).
19. W. A. H. M. VLAK, E. FRIKKEE, A. F. M. ARTS, AND H. W. DE WIJN, *J. Phys. C* **16,** L1015 (1983).
20. A. E. HUGHES, *Phys. Rev. B* **3,** 877 (1971).
21. C. R. BECKER, P. LAU, R. GEICK, AND V. WAGNER, *Phys. Status Solidi B* **67,** 653 (1975).
22. A. K. CHEETHAM, AND A. J. SKARNULIS, *Anal. Chem.* **53,** 1060 (1981).
23. H. M. RIETVELD, *J. Appl. Crystallogr.* **2,** 65 (1969).
24. G. E. BACON, "Neutron Diffraction," Oxford University Press, London/New York 1975.
25. A. J. JACOBSON, B. C. TOFIELD, AND B. E. F. FENDER, *J. Phys. C* **6,** 1615 (1973).
26. A. W. HEWAT, *Acta Crystallogr. A* **35,** 248 (1979).
27. D. A. O. HOPE, Ph.D. thesis, Oxford University, 1981.
28. D. A. O. HOPE, A. K. CHEETHAM, AND G. J. LONG, *Inorg. Chem.* **21,** 2804 (1982).
29. J. KANAMORI, *J. Appl. Phys.* **31,** 14S (1960).
30. J. B. GOODENOUGH, "Magnetism and the Chemical Bond," Wiley Interscience, New York, 1963.
31. F. GESMUNDO AND P. F. ROSSI, *J. Solid State Chem.* **8,** 287 (1973).
32. O. EVRARD, F. JEANNOT, AND J. M. LECUIRE, *Rev. Chim. Miner.* **9,** 463 (1972).
33. J. SAKURAI, W. J. L. BUYERS, R. A. COWLEY, AND G. DOLLING, *Phys. Rev.* **167,** 510 (1968).